J Mater Sci (2015) 50:6060–6065
DOI 10.1007/s10853-015-9155-1

Molten salt synthesis, energy transfer, and temperature quenching fluorescence of green-emitting β-$Ca_2P_2O_7$:Tb^{3+} phosphors

Yue Tian[1] · Yanhong Fang[2] · Bining Tian[3] · Cai'e Cui[1] · Ping Huang[1] · Lei Wang[1] · Huayu Jia[1] · Baojiu Chen[3]

Received: 17 March 2015 / Accepted: 4 June 2015 / Published online: 11 June 2015

Abstract Tb^{3+}-doped β-$Ca_2P_2O_7$ phosphors were successfully prepared via a simple surfactant-free molten salt method for the first time and characterized by X-ray diffraction (XRD), field emission scanning electron microscopy (SEM), and photoluminescence. The results of XRD and SEM suggest that the products belong to pure β-$Ca_2P_2O_7$ nanoparticles with average particle size of about 88.6 nm. Under the UV light excitation, the as-prepared β-$Ca_2P_2O_7$:Tb^{3+} phosphors exhibit green emission, which corresponds to the characteristic emissions of Tb^{3+} ion. The optimal doping concentration of Tb^{3+} ions in β-$Ca_2P_2O_7$ phosphors was confirmed to be abound 10 mol% and the exchange interaction is responsible for energy transfer between Tb^{3+} ions in β-$Ca_2P_2O_7$ phosphors. The fluorescent lifetime of $^5D_4$ level of Tb^{3+} in β-$Ca_2P_2O_7$ phosphors decreases with the increase of Tb^{3+} ions concentration because of self-generated quenching process, which was confirmed by Auzel's model. The thermal quenching behaviors of β-$Ca_2P_2O_7$:Tb^{3+} nanophosphors were also studied and the activation energy was deduced to be 0.265 eV.

✉ Yue Tian
tianyue@tyut.edu.cn

✉ Baojiu Chen
chenmbj@sohu.com

[1] Key Lab of Advanced Transducers and Intelligent Control System of Ministry of Education, College of Physics and Optoelectronic Engineering, Taiyuan University of Technology, Taiyuan 030024, People's Republic of China

[2] Naval Petty Officer Academy, Bengbu 233012, Anhui, People's Republic of China

[3] Department of Physics, Dalian Maritime University, Dalian 116026, Liaoning, People's Republic of China

Introduction

Rare earth (RE) ions doped luminescent materials have attracted considerable attention owing to their unique optical properties originating from the special electron configurations of 4f shell of the RE ions and have been widely applying in the fields of lighting, displays, lasers, etc. [1–4]. As one member of RE ions, it is well known that Tb^{3+} is frequently used as an activator of green-emitting materials due to its predominant $^5D_4 \rightarrow {}^7F_5$ transition [5]. To achieve excellent luminescent performance of Tb^{3+} ion, it is necessary to select proper host materials. Among various host materials, the phosphate is a promising host material due to its remarkable thermal, structural diversity and a rather short wavelength of optical absorption edge, for example, $Ca_2P_2O_7$ [6–9]. It is well known that $Ca_2P_2O_7$ exists in three different crystal structures including γ-, β-, and α-$Ca_2P_2O_7$, which depend on the temperature of firing [10]. RE-doped $Ca_2P_2O_7$ phosphors provide a novel flexible method for designing new luminescent materials. Currently, studies on $Ca_2P_2O_7$ phosphors have mainly been focused on Eu^{2+}-doped materials and materials co-doped with Eu^{2+} and another metal ion, which can emit blue or white light [7–9]. Moreover, these $Ca_2P_2O_7$ phosphors materials are usually synthesized by the solid-state reaction method, in which relatively high temperature and prolonged heating time are required. As a result, the size and morphology of the as-obtained $Ca_2P_2O_7$ phosphors are not uniform and regular. To the best of our knowledge, however, the report on luminescent properties of other RE ion-doped $Ca_2P_2O_7$ phosphor is rare. Especially, nanosized $Ca_2P_2O_7$ phosphors prepared via molten salt method has not been reported now.

The molten salt method has been proved to be one of the most convenient, effective, and environmental friendly

approaches for achieving single-phased nano- or micro-crystals at relatively lower temperature and shorter reaction time compared with the conventional solid-state reactions [11]. Therefore, this method has been extensively used for the preparation of electron ceramic powders and some other inorganic functional materials [12]. At the certain temperature, inorganic mixed salts, such as $NaNO_3$ and KNO_3, can melt into ionic liquids, which can be used as an effective chemical reaction medium to produce a high-temperature liquid environment for crystal growth. The fundamental basis of molten salt reactions is the use of different types of inorganic molten salts as the reaction medium. Moreover, the inorganic molten salts usually have several favorable physicochemical properties including a higher oxidizing potential, high mass transfer, high thermal conductivity, as well as relatively lower viscosities and densities, as compared with conventional solvents [13]. Therefore, the molten salt method is considered as one of the simplest, most versatile, and cost-effective approaches to obtain crystalline, chemically purified, single-phase powders at lower temperatures and often in overall shorter reaction times with little residual impurities as compared with conventional solid-state reactions. In recent years, many inorganic compounds have been synthesized through molten salt method, such as $NaLuF_4$ [11], $ZnWO_4$ [12], Gd_2MO_6 (M = W, Mo) [14], etc.

In this paper, Tb^{3+}-doped β-$Ca_2P_2O_7$ phosphors were prepared via molten salt method using $NaNO_3$–KNO_3 as the medium. X-ray diffraction (XRD) and scanning electron microscopy (SEM) results suggest that the as-prepared samples are pure phase of β-$Ca_2P_2O_7$. The optimal doping concentration of Tb^{3+} ions in $Ca_2P_2O_7$ phosphors was confirmed to be around 10 mol%. In addition, the energy transfer and thermal quenching behavior of Tb^{3+}-doped β-$Ca_2P_2O_7$ phosphors were studied in detail.

Experimental

Sample synthesis

Tb^{3+}-doped β-$Ca_2P_2O_7$ phosphors were prepared via molten salt process for the first time. In a typical procedure, the certain amounts of calcium nitrate, ammonia phosphate, terbium nitrate hexahydrate, sodium nitrate, and potassium nitrate (the molar ratio: $(1-x)$:1:x:50:25, where x = 0.5–12 mol%) were mixed and ground thoroughly in an agate mortar for about 30 min. After being ground, the as-obtained mixture was transferred into an alumina crucible with a lip and heated at 350 °C for 3 h. After cooling to room temperature naturally, the as-prepared sample was washed with distilled water and collected via centrifugation several times. Finally, the product was dried at 80 °C in air for 10 h.

Characterization

X-ray powder diffraction (XRD) of the as-prepared samples was performed on a Shimadzu XRD-6000 diffractometer with Cu $K_{\alpha 1}$ radiation (λ = 0.15406 nm). The XRD data were collected using a scanning mode in 2θ ranging from 10° to 60° with a step size of 0.02° and a rate of 4.0°/min. The morphology of the samples was observed by field emission scanning electron microscopy (FE-SEM, Hitachi S-4800). The excitation & emission spectra and fluorescent decays were recorded with a Hitachi F-4600 spectrophotometer equipped with a 150 W xenon lamp as excitation source. A homemade temperature control system was used to measure temperature-dependent emission spectra from 25 to 250 °C. The measuring and controlling accuracy of the temperature is about ±0.5 °C.

Results and discussion

Crystal structure of as-prepared samples

The typical XRD patterns for 0.5 and 10 mol% Tb^{3+}-doped β-$Ca_2P_2O_7$ phosphors are shown in Fig. 1. It can be found that all the diffraction peak positions from the 0.5 and 10 mol% Tb^{3+}-doped β-$Ca_2P_2O_7$ phosphors are well consistent with that of the pure tetragonal phase of $Ca_2P_2O_7$ with space group *P41(76)*, which was reported in JCPDS card with No. 71-2123. No extra diffraction peaks corresponding to any impurities are observed even in the sample with highest concentration of Tb^{3+}. This fact indicates that the tetragonal phase of $Ca_2P_2O_7$ polycrystals can be formed directly via simple molten salt process, and that the crystal structure of the products is influenced

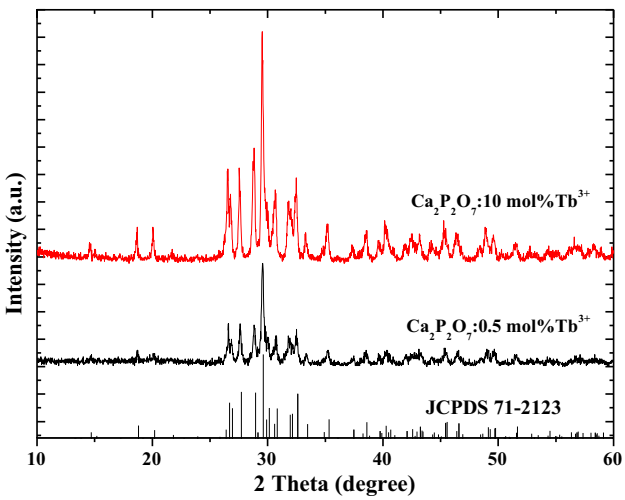

Fig. 1 XRD patterns of 0.5 and 10 mol% Tb^{3+}-doped β-$Ca_2P_2O_7$ phosphors

slightly by the introduction of Tb^{3+} ions. Herein, Tb^{3+} ions should substitute the sites of Ca^{2+} ions in β-$Ca_2P_2O_7$ host because of the similar ionic radius and Na^+ are K^+ ions may be used as charge compensators during the synthesis process. In addition, we can also see that the XRD peaks of the prepared samples are intense and sharp, suggesting that the products are crystallized well. This is in the favor of high efficient luminescence of RE ions as well.

SEM observations

Figure 2a and b shows the SEM images of 0.5 and 10 mol% Tb^{3+}-doped β-$Ca_2P_2O_7$ phosphors prepared using $NaNO_3$ and KNO_3 as molten salt. It can be seen that both of them present the similar morphology and size distribution. However, the size and morphology of the phosphors are not relatively uniform and regular. Meanwhile, some particles are agglomerated into bulk and the size range of particles is from 30 to 140 nm. By counting 100 identifiable particles not including the agglomerated bulk, the average particle size was estimated from the size distribution to be around 88.6 nm. Although the aggregation of particles is still observed though the molten salt method, the temperature is much lower than that of solid-state reaction and the reaction period is much shorter. Therefore, this can save a lot of energy resource.

Photoluminescent properties

The excitation spectra of the as-prepared β-$Ca_2P_2O_7$:-x mol% Tb^{3+} ($x = 0.5$–12) phosphors by monitoring 545 nm emission are shown in Fig. 3. It can be found that the excitation spectra have the similar profiles except for the intensity and are composed of two parts: One is a broad band ranging from 200 to 275 nm, which corresponds to the 4f → 5d of Tb^{3+} transitions and the other is a set of some weak lines, which can be attributed to the f–f transitions within the $4f^8$ configuration of Tb^{3+} ion [15]. Under the 375 nm excitation, the as-prepared β-$Ca_2P_2O_7$:-x mol%Tb^{3+} ($x = 0.5$–12) phosphors exhibit green emission and the typical emission spectra are shown in Fig. 4. The emission peaks located at 490, 545, 585, and 623 nm can be observed, which correspond to the $^5D_4 \rightarrow {}^7F_6$, $^5D_4 \rightarrow {}^7F_5$, $^5D_4 \rightarrow {}^7F_4$, and $^5D_4 \rightarrow {}^7F_3$ transitions of Tb^{3+}, respectively. The green emission of $^5D_4 \rightarrow {}^7F_5$ transition is dominant in the emission spectra. Therefore, the samples exhibit green color under the UV light excitation. The emissions from the $^5D_3$ level cannot be observed even in the samples with lower Tb^{3+} concentration (0.5 mol%), which is due to the relative high phonon energy of host and unnegligible cross-relaxation effect, i.e., $^5D_3 + {}^7F_6 \rightarrow {}^5D_4 + {}^7F_0$ [15].

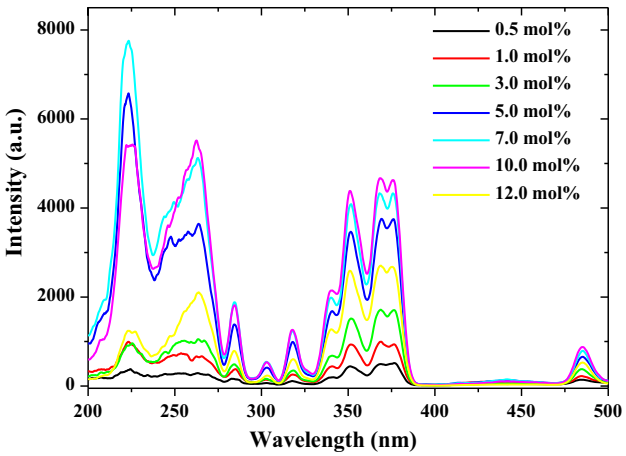

Fig. 3 Excitation spectra of Tb^{3+}-doped β-$Ca_2P_2O_7$ phosphors by monitoring at 545 nm (Color figure online)

The doping concentration of luminescent activators is an important factor that can influence the phosphor performance greatly. Therefore, it is necessary to confirm the

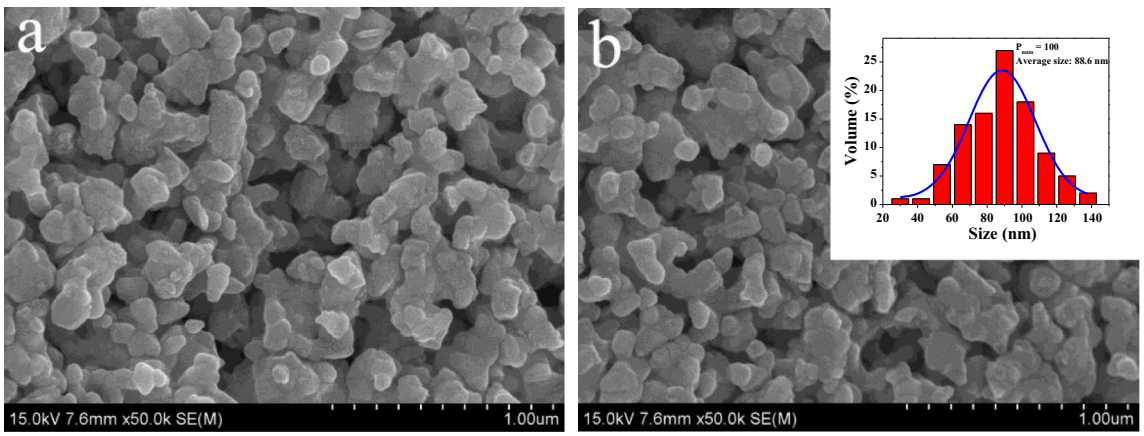

Fig. 2 SEM images of 0.5 and 10 mol% Tb^{3+}-doped β-$Ca_2P_2O_7$ phosphors. The *inset* of (**b**) shows particle size distribution histograms for the Tb^{3+}-doped β-$Ca_2P_2O_7$ sample

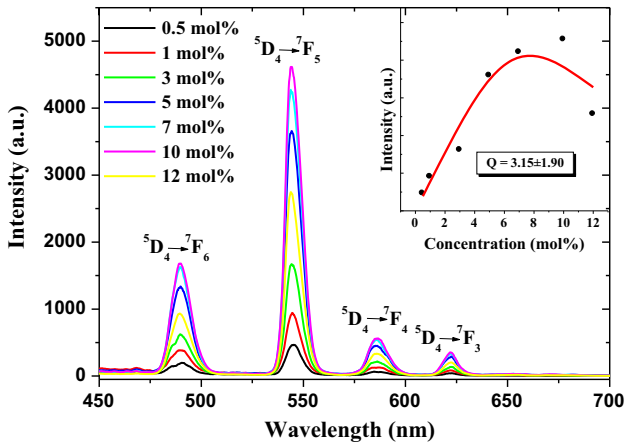

Fig. 4 Emission spectra of Tb^{3+}-doped β-$Ca_2P_2O_7$ phosphors excited upon 375 nm. The inset is dependence of $^5D_4$ emission intensity on Tb^{3+} ions doping concentration and solid line is fitting curve (Color figure online)

optimal doping concentration for obtaining strongest emission intensity. The inset in Fig. 4 shows the dependence of the integrated emission intensity of $^5D_4 \rightarrow {}^7F_5$ transition on Tb^{3+} concentration in β-$Ca_2P_2O_7$ phosphors. It can be seen that the integrated emission intensity of $^5D_4 \rightarrow {}^7F_5$ transition increases firstly with the increase of Tb^{3+} doping concentration and then reaches its maximum at around 10 mol% Tb^{3+}. When the doping concentration of Tb^{3+} ions is more than 10 mol%, the emission intensity decreases. Namely concentration quenching occurs. Therefore, the optimal concentration of Tb^{3+} in β-$Ca_2P_2O_7$ phosphors can be confirmed to be about 10 mol%.

Energy transfer and self-generated quenching of Tb^{3+} in β-$Ca_2P_2O_7$

Van Uitert has developed a phenomenological model to explain the relationship between the luminescent intensity and the concentration of luminescent center, which can be written by [16, 17]

$$I(C) = \frac{C}{K[1 + \beta C^{Q/3}]}, \quad (1)$$

where C is doping concentration of Tb^{3+} ions in the present case; K and β are constants for a certain system; Q represents the interaction type between luminescence center and quenching center, here $Q = 3$, 6, 8, or 10, indicating, respectively, the exchange interaction, electric dipole–dipole (D–D), electric dipole-quadrupole (D–Q), and electric quadrupole–quadrupole (Q–Q) interactions. In order to understand the energy transfer mechanism between Tb^{3+} ions in β-$Ca_2P_2O_7$ phosphors, the Eq. (1) was used to fit the experimental data in inset in Fig. 4. It can be found that Eq. (1) can fit well with the experimental data, and the Q value was deduced from the fitting process to be 3.15, which suggests the exchange interaction is responsible for energy transfer of the $^5D_4$ level of Tb^{3+} in β-$Ca_2P_2O_7$ phosphors. Considering that luminescence quenching is caused by the energy transfer within the same RE ions, the critical distance (R_C) can be estimated in terms of the equation developed by Blasse [18]

$$R_c = 2\left(\frac{3V}{4\pi X_c N}\right)^{1/3}, \quad (2)$$

where V is the volume of the unit cell, and X_c is the critical concentration, which is the concentration of Tb^{3+} ions at the half of strongest emission intensity. Herein, X_c is about 12 mol%. N is the number of available crystallographic sites occupied by the activator ions in the unit cell. The values of V and N for the tetragonal $Ca_2P_2O_7$ are 1078.65 Å^3 and 8, respectively (JCPDS 71-2123). Therefore, the R_C for Tb^{3+} in β-$Ca_2P_2O_7$ phosphor is about 2.88 Å.

Figure 5 shows the fluorescent decay curves of the $^5D_4$ level of Tb^{3+} ions in β-$Ca_2P_2O_7$:x mol% Tb^{3+} ($x = 0.5$–12) phosphors under the 375 nm excitation. It can be seen that all these decays follow single-exponential function, indicating that the energy transfer between Tb^{3+} ions is an energy migration process [19, 20]. In this case, the excitation energy quickly transfers between Tb^{3+} ions, and finally is captured by the quenchers, which may be the lattice defects or unintended dopants. The decay time constants were derived via single-exponential fitting and are also listed in inset in Fig. 5. The dotted circles in inset in Fig. 5 show the dependence of average fluorescent lifetime on the doping concentration of Tb^{3+}. It can be found that with the increase of Tb^{3+} concentration the lifetime of the $^5D_4$ level of Tb^{3+} decreases. It is well

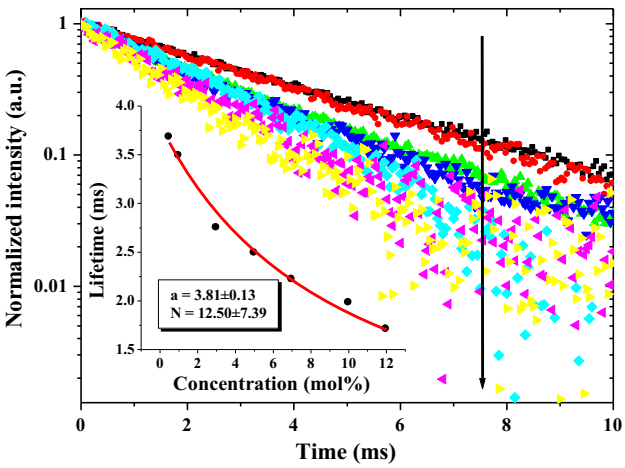

Fig. 5 Fluorescent curves of Tb^{3+}-doped β-$Ca_2P_2O_7$ phosphors ($\lambda_{ex} = 375$, $\lambda_{em} = 543$). The inset is dependence of $^5D_4$ lifetime on Tb^{3+} ions doping concentration and solid line is fitting curve

known that there is no energy transfer quenching $^5D_4$ level of Tb^{3+}. Therefore, the self-generated quenching process should be a dominant mechanism for the lifetime variation. The self-generated quenching process occurs, usually, in the instance that the average distance between activators is short enough, and the energy transfer from the studied level does not exist, which has been proved above [20]. Auzel has developed a physical model to describe the dependence of fluorescent lifetime on the doping concentration for the self-generated quenching system, where their relationship can be mathematically expressed as [21]

$$\tau(c) = \frac{\tau_0}{1 - \frac{c}{c_0} e^{-\frac{N}{3}}}, \tag{3}$$

where $\tau(c)$ is fluorescent lifetime at concentration c, τ_0 is radiative transition lifetime, c_0 is a constant with the same dimension as the concentration c, and N is the number of phonon required for quenching the studied level via cascade multiphonon process. The fluorescent lifetime data were fitted by Eq. (3) and the solid line in inset in Fig. 5 shows the fitting curve. As seen in Fig. 5, the experimental data can be fitted well by Eq. (3). In the fitting process, the N value is confirmed to be 12.5, indicating that the $^5D_4$ level can be quenched via nonradiative relaxation by generating about 13 phonons. It is known that the energy difference between $^5D_4$ and $^7F_0$ is around 14784 cm^{-1}, which is around 14 times as the highest phonon energy (1051 cm^{-1}) of the host [22]. Therefore, it requires 14 phonons at least to bridge these two levels, which is close to fitting value of N. This fact means that Auzel's model can well explain the self-generated quenching process of Tb^{3+} in β-$Ca_2P_2O_7$ phosphors. Additionally, the intrinsic radiative transition lifetime τ_0 of $^5D_4$ level of Tb^{3+} ions in β-$Ca_2P_2O_7$ phosphors was also obtained to be 3.81 ms via the fitting process. The internal quantum efficiency can be written by

$$\eta = \frac{\tau_s}{\tau_0}, \tag{4}$$

where τ_s is the measured fluorescence lifetime. Therefore, the maximally external quantum efficiency is 96.59 % for the 0.5 mol% Tb^{3+}-doped sample. The external quantum efficiency decreases to 44.88 % when doping concentration increases to 12 mol% because of the increase of the nonradiative transition rate.

Thermal quenching behavior

Usually, the spectral properties of luminescence materials are temperature dependent and thermal effect of luminescence materials is also an important aspect of spectroscopic investigations. Comprehensively understanding the thermal deterioration and fluorescence temperature quenching of the phosphors is beneficial to improve phosphors' performance via material design and synthesis. To examine the thermal performance of all the as-prepared β-$Ca_2P_2O_7$ phosphors, their emission spectra were measured at temperatures ranging from 298 K to 523 K upon 375 nm excitation. As an example, the emission spectra for β-$Ca_2P_2O_7$:10 mol%Tb^{3+} phosphor excited at different temperature are shown in Fig. 6. It can be found that the emissions from the $^5D_4$ level decrease with the increase of temperature. Namely thermal quenching occurs. It is known that the luminescent ion can go back to the ground state via thermal quenching. In other words, it can reach the ground state when the excited state and the ground state energy curves cross at an energy which is thermally accessible from the relaxed excited state. It is assumed that the nonradiative rate k_{nr} can be expressed as [23]

$$k_{nr} = Ae^{-\frac{\Delta E}{kT}}, \tag{5}$$

where A is a constant, k is Boltzmann's constant, and ΔE is the activation energy for the thermal quenching process. Thus, the emission intensity decreases due to the increase of probability of nonradiative transition with temperature. According to Eq. (5), a lower value of ΔE means a more rapid nonradiative rate at a given temperature. The Arrhenius equation can be used to describe the temperature dependence of the luminescent intensity [23–25].

$$I(T) = \frac{I_0}{1 + Ce^{-\frac{\Delta E}{kT}}}, \tag{6}$$

where I_0 is the initial luminescent intensity, $I(T)$ is the luminescent intensity at given temperature T, C is a constant, k is Boltzmann's constant, and ΔE is the activation energy for the thermal quenching process. The inset in

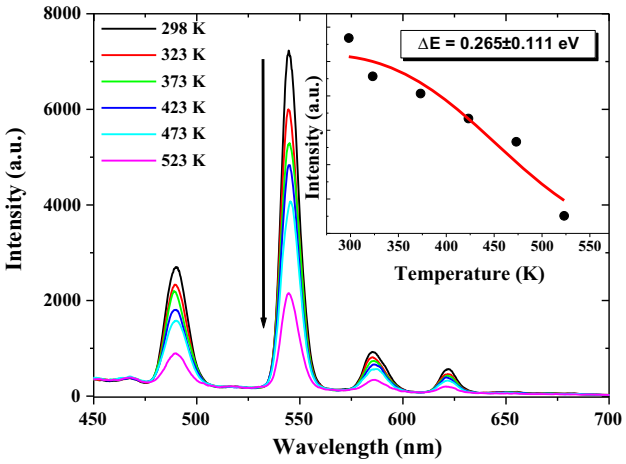

Fig. 6 Emission spectra of β-$Ca_2P_2O_7$:10 mol%Tb^{3+} phosphors excited upon 375 nm at different temperature. The inset is dependence of $^5D_4$ emission intensity on ambient temperature and solid line is fitting curve (Color figure online)

Fig. 6 shows the dependence of integrated emission intensity of the $^5D_4$ level on temperature. Equation (6) is used to nonlinearly fit the experimental data of thermal quenching; the solid line shows the fitting curve. It can be found that the experimental data are fitted well with Eq. (6). From the fitting process, the activation energy was confirmed to be 0.265 eV.

Conclusion

In conclusion, Tb^{3+}-doped β-$Ca_2P_2O_7$ phosphors with average size of 88.6 nm have been successfully prepared via simple and environmental friendly molten salts method using $NaNO_3$ and KNO_3 as the medium. The luminescent properties of Tb^{3+}-doped β-$Ca_2P_2O_7$ phosphors have been studied as well. The results suggested that the optimal doping concentration of Tb^{3+} ions in β-$Ca_2P_2O_7$ phosphors is about 10 mol% and a critical distance of 2.88 Å was obtained for energy transfer between Tb^{3+} ions. In addition, it was found that the self-generated quenching process is responsible for concentration quenching of Tb^{3+} ions in β-$Ca_2P_2O_7$ phosphors according to the Auzel's model and the intrinsic radiative transition lifetime τ_0 of $^5D_4$ level was deduced to be 3.81 ms. The luminescent intensities of Tb^{3+}-doped β-$Ca_2P_2O_7$ phosphors decrease with the increase of ambient temperature because of temperature quenching and the activation energy was confirmed to be 0.265 eV.

Acknowledgements This work was partially supported by National Natural Science Foundation of China (NSFC, Grant Nos. 11374044 and 51302182), The National High Technology Research and Development Program ("863" Program) of China (2015AA016901), The Qualified Personnel Foundation of Taiyuan University of Technology (QPFT) (No: tyut-rc201361a), and The Program for the outstanding Innovative Teams of Higher Learning Institutions of Shanxi.

References

1. Tian Y, Qi XH, Wu XW, Hua RN, Chen BJ (2009) Luminescent properties of $Y_2(MoO_4)_3$:Eu^{3+} red phosphors with flowerlike shape prepared via coprecipitation method. J Phys Chem C 113:10767–10772
2. Lakshminarayana G, Qiu JR (2009) Photoluminescence of Eu^{3+}, Tb^{3+} and Tm^{3+} doped transparent SiO_2-Al_2O_3-LiF-GdF_3 glass ceramics. J. Alloys Compd 476:720–727
3. Lakshminarayana G, Buddhudu S (2007) Spectral analysis of Eu^{3+} and Tb^{3+}: B_2O_3-ZnO-PbO glasses. Mater Chem Phys 102:181–186
4. Lakshminarayana G, Qiu JR (2009) Photoluminescence of Pr^{3+}, Sm^{3+} and Dy^{3+}-doped SiO_2-Al_2O_3-BaF_2-GdF_3 glasses. J. Alloys Compd 476:470–476
5. Han LL, Wang YH, Wang YZ, Zhang J, Tao Y (2013) Observation of efficient energy transfer from host to rare-earth ions in $KBaY(BO_3)_2$:Tb^{3+} phosphor for plasma display panel. J. Alloys Compd 551:485–489
6. Yonesaki Y (2013) Sensitized red luminescence from Mn^{2+}-doped olgite-type phosphate. J Solid State Chem 197:166–171
7. Hao ZD, Zhang JH, Zhang X, Lu SZ, Luo YS, Ren XG, Wang XJ (2008) Phase dependent photoluminescence and energy transfer in $Ca_2P_2O_7$:Eu^{2+}, Mn^{2+} phosphors for white LEDs. J Lumin 128:941–944
8. Pang R, Li CY, Zhang S, Su Q (2009) Luminescent properties of a new blue long-lasting phosphor $Ca_2P_2O_7$:Eu^{2+}, Y^{3+}. Mater Chem Phys 113:215–218
9. Hao ZD, Zhang JH, Zhang X, Sun XY, Luo YS, Lu SZ, Wang XJ (2007) White light emitting diode by using α-$Ca_2P_2O_7$:Eu^{2+}, Mn^{2+} phosphor. Appl. Phys. Lett. 90:261113-1–261113-3
10. Bian JJ, Kim DW, Hong KS (2004) Phase transformation and sintering behavior of $Ca_2P_2O_7$. Mater Lett 58:347–351
11. Niu N, Yang PP, He F, Zhang X, Gai SL, Li CX, Lin J (2012) Tunable multicolor and bright white emission of one-dimensional $NaLuF_4$:Yb^{3+}, Ln^{3+} (Ln = Er, Tm, Er/Tm, Tm/Ho) microstructures. J Mater Chem C 22:10889–10899
12. Yan B, Lei F (2010) Molten salt synthesis, characterization and luminescence of $ZnWO_4$:Eu^{3+} phosphors. J Alloys Compd 507:460–464
13. Volkov SV (1990) Chemical reactions in molten salts and their classification. Chem Soc Rev 19:21–28
14. Lei F, Yan B, Chen HH, Zhao JT (2009) Molten salt synthesis, characterization, and luminescence properties of Gd_2MO_6:Eu^{3+} (M = W, Mo) phosphors. J Am Ceram Soc 92:1262–1267
15. Tian Y, Chen BJ, Tian BN, Sun JS, Li XP, Zhang JS, Cheng LH, Zhong HY, Zhong H, Meng QY, Hua RN (2012) Ionic liquid-assisted hydrothermal synthesis of dendrite-like $NaY(MoO_4)_2$:-Tb^{3+} phosphor. Phys B 407:2556–2559
16. Van Uitert LG (1967) Characterization of energy transfer interactions between rare earth ions. J Electrochem Soc 114:1048–1053
17. Tian Y, Chen BJ, Tian BN, Hua RN, Sun JS, Cheng LH, Zhong HY, Li XP, Zhang JS, Zheng YF, Yu TT, Huang LB, Meng QY (2011) Concentration-dependent luminescence and energy transfer of flower-like $Y_2(MoO_4)_3$:Dy^{3+} phosphor. J Alloy Compd 509:6096–6101
18. Blasse G (1986) Energy transfer between inequivalent Eu^{3+} ions. J Solid State Chem 62:207
19. van der Ziel JP, Kopf L, Van Uitert LG (1972) Quenching of Tb^{3+} luminescence by direct transfer and migration in aluminum garnets. Phys Rev B 6:615–623
20. Tian Y, Chen BJ, Hua RN, Sun JS, Cheng LH, Zhong HY, Li XP, Zhang JS, Zheng YF, Yu TT, Huang LB, Yu HQ (2011) Opitical transition, electron-phonon coupling and fluorescent quenching of $La_2(MoO_4)_3$:Eu^{3+} phosphor. J Appl Phys 109:053511-1–053511-6
21. Auzel F (2002) A fundamental self-generated quenching center for lanthanide-doped high purity solids. J Lumin 100:125–130
22. Cornilsen BC, Condrate RA Sr (1979) The vibrational spectra of β-$Ca_2P_2O_7$ and γ-$Ca_2P_2O_7$. J Inorg Nucl Chem 41:602–605
23. Tian BN, Chen BJ, Tian Y, Sun JS, Li XP, Zhang JS, Zhong HY, Cheng LH, Hua RN (2012) Concentration and temperature quenching mechanisms of Dy^{3+} luminescence in $BaGd_2ZnO_5$ phosphors. J Phys Chem Solid 73:1314–1319
24. Tian BN, Chen BJ, Tian Y, Li XP, Zhang JS, Sun JS, Zhong HY, Cheng LH, Fu SB, Zhong H, Wang YZ, Zhang XQ, Xia HP, Hua RN (2013) Excitation pathway and temperature dependent luminescence in color tunable $Ba_5Gd_8Zn_4O_{21}$ phosphors. J Mater Chem C 1:2338–2344
25. Tian Y, Chen BJ, Hua RN, Yu NS, Liu BQ, Sun JS, Cheng LH, Zhong HY, Li XP, Zhang JS, Tian BN, Zhong H (2012) Self-assembled 3D flower-shaped $NaY(WO_4)_2$:Eu^{3+} microarchitectures: microwave-assisted hydrothermal synthesis, growth mechanism and luminescent properties. CrystEngComm 14:1760–1769